

# Probing the nuclear deformation with three-particle asymmetric cumulant in RHIC isobar runs

Shujun Zhao<sup>a,b</sup>, Hao-jie Xu<sup>b,\*</sup>, Yu-Xin Liu<sup>a,c,d,\*</sup>, Huichao Song<sup>a,c,d,\*</sup>

<sup>a</sup>Department of Physics and State Key Laboratory of Nuclear Physics and Technology, Peking University, Beijing 100871, China

<sup>b</sup>School of Science, Huzhou University, Huzhou, Zhejiang 313000, China

<sup>c</sup>Collaborative Innovation Center of Quantum Matter, Beijing 100871, China

<sup>d</sup>Center for High Energy Physics, Peking University, Beijing 100871, China

## Abstract

$^{96}_{44}\text{Ru}+^{96}_{44}\text{Ru}$  and  $^{96}_{40}\text{Zr}+^{96}_{40}\text{Zr}$  collisions at  $\sqrt{s_{\text{NN}}} = 200$  GeV provide unique opportunities to study the geometry and fluctuations raised from the deformation of the colliding nuclei. Using iEBE-VISHNU hybrid model, we predict  $ac_2\{3\}$  ratios between these two collision systems and demonstrate that the ratios of  $ac_2\{3\}$ , as well as the ratios of the involving flow harmonics and event-plane correlations, are sensitive to quadrupole and octupole deformations, which could provide strong constrains on the shape differences between  $^{96}\text{Ru}$  and  $^{96}\text{Zr}$ .

## 1. Introduction

Anisotropic flow observed in heavy-ion collisions at Relativistic Heavy-Ion Collider (RHIC) and Large Hadron Collider (LHC) indicate that the created quark-gluon-plasma (QGP) is a strongly coupled system with small specific shear viscosity [1–9]. Hydrodynamic simulations have successfully described the collective expansion of the QGP fireball and studied various flow observables at RHIC and the LHC [10–19]. After the hydrodynamic evolution, the initial stage geometry and fluctuations are translated into final stage correlations described by various flow observables such as different order flow harmonics, correlations between flow harmonics, event-plane correlations, etc. [19–29]. On the other hand, these flow observables raised from the collective expansion also depend on the properties of the QGP and the details of the initial profiles. The RHIC isobar runs with  $^{96}_{40}\text{Zr}+^{96}_{40}\text{Zr}$  and  $^{96}_{44}\text{Ru}+^{96}_{44}\text{Ru}$  collisions at  $\sqrt{s_{\text{NN}}} = 200$  GeV provide unique opportunities to probe the nuclear structure of the colliding nuclei from the initial stage, since the uncertainties from the bulk properties of the QGP can be largely reduced through the observable ratios between the two collision systems [30, 31].

The  $^{96}_{40}\text{Zr}+^{96}_{40}\text{Zr}$  and  $^{96}_{44}\text{Ru}+^{96}_{44}\text{Ru}$  collisions at  $\sqrt{s_{\text{NN}}} = 200$  GeV originally aimed to search the chiral magnetic effect (CME). The observed differences in multiplicity distribution ( $N_{\text{ch}}$ ) and anisotropic flow harmonics between these two systems ruin the premise that isobar collisions can help identify the CME with enough precision [32, 33], but provide a novel way to constrain the nuclear deformation from heavy ion collisions [34]. For the typical initial profile construction for A+A collisions, the

Woods-Saxon distribution for the nuclear density is written as:

$$\rho = \frac{\rho_0}{1 + \exp[(r - R)/a]}, \quad (1)$$

$$R = R_0 \left( 1 + \beta_2 Y_2^0(\theta, \phi) + \beta_3 Y_3^0(\theta, \phi) + \dots \right), \quad (2)$$

where  $a$  is the diffuseness parameter,  $R_0$  is the radius parameter, and  $\beta_2$  ( $\beta_3$ ) is the parameter for quadrupole (octupole) deformation. In the central collisions with impact parameter  $b = 0$  fm, the deformed nuclei can naturally contribute geometric anisotropy of the overlap area, leading to larger anisotropic flow than the one from spherical nuclei collisions [35–38]. For the central isobar collisions at RHIC, the observed difference for elliptic flow  $v_2$  and triangle flow  $v_3$  between the two collision systems indicate a larger quadrupole deformation for  $^{96}\text{Ru}$  and a larger octupole deformation for  $^{96}\text{Zr}$  [30, 39]. In non-central collisions,  $v_2$  also depends on the diffuseness parameter  $a$  [40], and the non-trivial bump structure of  $v_2$  ratio as a function of centrality indicate a thick halo-type neutron skin thickness for  $^{96}\text{Zr}$  [30], consisting with the predictions from energy density functional theory (DFT) [32, 41]. Recently, more observables have been proposed to probe the nuclear structure in relativistic isobar collisions, such as the differences in multiplicity distribution [34], net charge number ( $\Delta Q$ ) [42], mean transverse momentum ( $\langle p_T \rangle$ ) [31],  $\langle p_T \rangle$  fluctuations [43], and spectator neutrons [44], etc. Benefiting from huge statistics and the strategy to reduce systematic uncertainties in experiment [30], the isobar collisions are expected to provide more precise measurements of neutron skin thickness and nuclear deformations.

Compared with lower order flow harmonics, higher order flow harmonics, as well as the correlations between different flow harmonics are expected to be sensitive to the initial state deformations [24], which provide more information for precisely probing the nuclear structure differences between the two isobar systems. The flow harmonics and their correla-

\*Corresponding author

Email addresses: haojie.xu@zjhu.edu.cn (Hao-jie Xu), yxliu@pku.edu.cn (Yu-Xin Liu), huichaosong@pku.edu.cn (Huichao Song)

Table 1: The iEBE-VISHNU parameters are roughly tuned to reproduce the multiplicity and flow observables reported by the STAR collaboration [30]. A detailed description of the following parameters can be found in Ref [45].

Initial condition/Preeq.		QGP medium	
Norm	6.6 GeV	$(\eta/s)_{\min}$	0.134
$p$	0.0	$(\eta/s)_{\text{slope}}$	$1.6 \text{ GeV}^{-1}$
$\sigma_{\text{flut}}$	0.91	$(\eta/s)_{\text{crv}}$	-0.29
$r_{\text{cp}}$	0.88 fm	$(\zeta/s)_{\text{max}}$	0.052
$n_c$	6.0	$(\zeta/s)_{\text{width}}$	0.024 GeV
$w_c$	0.36 fm	$(\zeta/s)_{T_{\text{peak}}}$	0.175 GeV
$d_{\text{min}}$	0.4 fm	$T_{\text{switch}}$	0.151 GeV
$\tau_{\text{fs}}$	0.37 fm/c		

tions can be calculated by the multi-particle azimuthal correlations [20, 21]:

$$\langle m \rangle_{n_1, n_2, \dots, n_m} \equiv \langle e^{i(n_1\varphi_{k_1} + n_2\varphi_{k_2} + \dots + n_m\varphi_{k_m})} \rangle, \quad (3)$$

Here  $\langle \dots \rangle$  denotes the sum of all particles of interest (POI) in a given event. The three-particle asymmetric cumulant can be calculated with [23–25, 27, 28]:

$$\text{ac}_2\{3\} \equiv \langle \langle 3 \rangle_{2,2,-4} \rangle = \langle \langle e^{i(2\varphi_1 + 2\varphi_2 - 4\varphi_3)} \rangle \rangle \quad (4)$$

Here  $\langle \langle \dots \rangle \rangle$  indicates the average of  $\langle \dots \rangle$  over an ensemble of events.  $\text{ac}_2\{3\}$  is sensitive to the flow magnitudes and event-plane correlations. It is also directly related to the nonlinear response between the second and fourth order flow vector, which can also be used to extract the corresponding nonlinear response coefficients [24].

We will show in this work that the  $\text{ac}_2\{3\}$  ratios in isobar collisions are very sensitive to the deformation of the colliding nuclei. In the absence of non-flow effects, the  $\text{ac}_2\{3\}$  can be written as [24]

$$\text{ac}_2\{3\} = \langle v_2^2 v_4 \cos 4(\Phi_2 - \Phi_4) \rangle, \quad (5)$$

where  $\Phi$  is the event-plane of the related flow harmonic. Inherited from  $v_2$ ,  $\text{ac}_2\{3\}$  is sensitive to the deformation of the colliding nuclei [30, 39, 41]. We will show that the normalized asymmetric cumulant

$$\text{nac}_2\{3\} \equiv \frac{\text{ac}_2\{3\}}{\sqrt{(2v_2\{2\})^4 - v_2\{4\}^4} v_4\{2\}^2} \quad (6)$$

is also sensitive to the nuclear deformation, even if the contributions from single flow harmonics have been scaled out. Here,

$$\begin{aligned} v_2\{2\}^2 &= \langle \langle 2 \rangle_{2,-2} \rangle, \\ v_4\{2\}^2 &= \langle \langle 2 \rangle_{4,-4} \rangle, \\ v_2\{4\}^4 &= 2v_2\{2\}^4 - \langle \langle 4 \rangle_{2,2,-2,-2} \rangle. \end{aligned} \quad (7)$$

In this letter, we will implement iEBE-VISHNU hybrid model to calculate the flow observables and demonstrate that the nuclear deformation not only influences the magnitude of anisotropic flow but also their correlations, which can be reflected by  $\text{ac}_2\{3\}$  and  $\text{nac}_2\{3\}$  correlations. Specifically, the effect on flow harmonics is amplified in the ratio of  $\text{ac}_2\{3\}$ , and

Table 2: WS parameterizations (radius parameter  $R_0$ , diffuseness parameter  $a$ , and deformation parameters  $\beta_2, \beta_3$ ) of the  $^{96}\text{Ru}$  and  $^{96}\text{Zr}$  nuclear density distributions with different nuclear deformations, followed by the procedure given in Ref. [42]. The quoted values for  $R_0$  and  $a$  are in fm.

	$\beta_2$	$\beta_3$	$R_0$	$a$
Ru-para-I	0.12	0.00	5.093	0.487
Ru-para-II	0.16	0.00	5.093	0.471
Zr-para-I	0.00	0.16	5.021	0.524
Zr-para-II	0.00	0.20	5.021	0.517

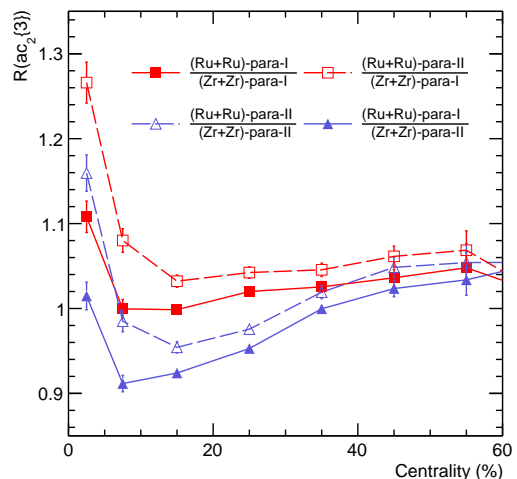


Figure 1: The centrality dependent  $R(\text{ac}_2\{3\})$  in relativistic isobar collisions, obtained from iEBE-VISHNU simulations. The standard Q-cumulant method is used for charged particles with  $0.2 < p_T < 2 \text{ GeV}/c$  and  $|\eta| < 2$ .

the residual effect from even-plane correlation is reflected by the ratio of  $\text{nac}_2\{3\}$ , where the ratio is defined as:

$$R(X) \equiv \frac{X_{\text{RuRu}}}{X_{\text{ZrZr}}}. \quad (8)$$

## 2. The model

In this paper, we implement iEBE-VISHNU to calculate the asymmetric cumulant  $\text{ac}_2\{3\}$  and the related flow observables in relativistic isobar collisions at  $\sqrt{s_{\text{NN}}} = 200 \text{ GeV}$ . iEBE-VISHNU [46, 47] is an event-by-event hybrid model that combines (2+1) dimensional viscous hydrodynamics [48, 49] to describe the expansion of the QGP and the hadron cascade model (UrQMD) to simulate the evolution of the subsequent hadronic matter [50, 51]. The initial condition of the collision is simulated by the Trento model [17, 52] with the given nuclear density distribution described by Eq. (1). The parameters for the iEBE-VISHNU simulation are listed in Tab. 1, which are tuned to roughly reproduce the multiplicity and flow observables measured in experiment [30]. A more detailed description of those parameters can be found in Ref [45].

The nuclear densities with deformation for  $^{96}\text{Ru}$  and  $^{96}\text{Zr}$  have been obtained in Ref. [31], using DFT calculations with the slope parameter of symmetry energy  $L(\rho_c) = 47.3 \text{ MeV}$ . The previous experiments about nuclear structure indicate that

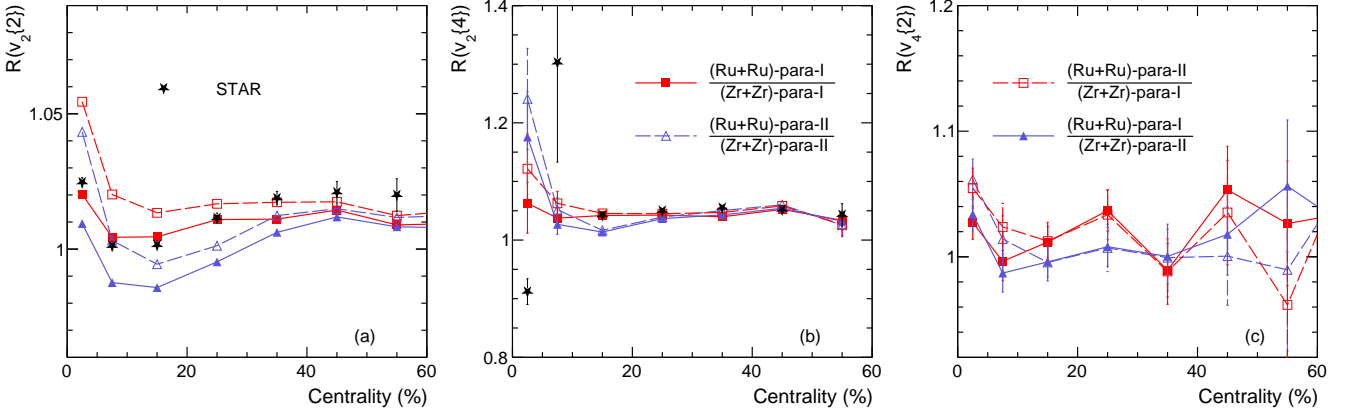


Figure 2: The centrality dependent (a)  $R(v_2\{2\})$ , (b)  $R(v_2\{4\})$  and (c)  $R(v_4\{2\})$  calculated by iEBE-VISHNU model with different sets of nuclear deformations. The flow harmonics are calculated by the standard Q-cumulant method with  $0.2 < p_T < 2$  GeV/c and  $|\eta| < 2$ . The data are taken from [30].

$\beta_{2,Ru} = 0.16$  with negligible octupole deformation and  $\beta_{3,Zr} = 0.20$  with negligible quadrupole deformation. However, recent hydrodynamic simulations on relativistic isobar collisions indicate that those values are overestimated [53]. We therefore choose another set of deformation factors for both  $^{96}\text{Ru}$  and  $^{96}\text{Zr}$ , i.e.  $\beta_{2,Ru} = 0.12$  and  $\beta_{3,Zr} = 0.16$ . We found that this can give a better description of elliptic flow ratio  $R(v_2)$  and triangle flow ratio  $R(v_3)$ , although the motivation of this study is not focus on quantitative prediction of flow ratios. The Woods-Saxon parameter sets for different deformation factors are listed in Tab. 2

In this study, the azimuthal correlations are calculated using the standard Q-cumulant method [20] with  $Q_n \equiv \langle e^{in\varphi} \rangle$ . All charged particles with  $0.2 < p_T < 2$  GeV/c are used. To reduce statistical uncertainties, an  $|\eta| < 2$  pseudorapidity cut is used. iEBE-VISHNU simulations contain part of the non-flow effect from resonance decays. While the standard Q-cumulant method can not fully reduce the non-flow effect, especially for the  $ac_2\{3\}$  which has a large non-flow subtraction method dependence [27, 28]. The large pseudorapidity cut used in this study can reduce the non-flow contributions to some extent, and we will discuss this in the next section.

### 3. Results and discussions

Figure 1 shows the ratio of  $ac_2\{3\}$ ,  $R(ac_2\{3\})$ , as a function of centrality in isobar collisions at  $\sqrt{s_{NN}}=200$  GeV, calculated from iEBE-VISHNU model. The comparison of  $R(ac_2\{3\})$  at most central collisions with different combination of the deformation parameters  $\beta_2$  and  $\beta_3$  demonstrates that  $R(ac_2\{3\})$  is sensitive to the nuclear deformation. The trend is similar to the one of  $R(v_2\{2\})$  as shown in Fig. 2(a), which decreases from most central to semi-central collision and then increases from semi-central to peripheral collisions. The large  $R(ac_2\{3\})$  and  $R(v_2\{2\})$  in the most central collisions are mostly due to the large quadrupole deformation in  $^{96}\text{Ru}$  [39], while the enhancement trend from semi-central to peripheral collisions are due to the thick halo-type neutron skin in  $^{96}\text{Zr}$  [41]. The octupole deformation in  $^{96}\text{Zr}$  give some contributions to  $R(ac_2\{3\})$

and  $R(v_2\{2\})$  in the most central collision, and lead to the valley structure in semi-central collisions [39]. Compared with  $R(v_2\{2\})$ ,  $R(ac_2\{3\})$  is more sensitive to nuclear deformation and contains more information on flow fluctuations and correlations. Description of their sensitivities on the nuclear structure at a quantitative level can help us to precisely constrain the nuclear deformation factors in isobar collisions. Note that the data of  $R(v_2\{2\})$  in Fig.2 (a) prefer  $\beta_{2,Ru} = 0.12$  and  $\beta_{3,Zr} = 0.16$ . While, we should also emphasis that this paper is not aimed to precisely describe the flow data in isobar collisions. More sophisticated extractions of the deformation parameters will be given in the following study [54].

Besides  $v_2\{2\}$ ,  $v_2\{4\}$  and  $v_4\{2\}$  also contribute to  $ac_2\{3\}$ . Due to flow fluctuations,  $v_2\{2\}$  from the two-particle correlation is larger than  $v_2\{4\}$  from the four-particle correlation for different collision systems. However, as shown in Fig. 2(a) and (b), the ratios  $R(v_2\{2\})$  and  $R(v_2\{4\})$  in isobar collisions present opposite behavior as observed in experiment [30], which indicates the importance of initial state deformation and fluctuations [55]. Note that the  $R(v_2\{4\})$  and  $R(v_4\{2\})$  in the most central collisions also depend on the deformation. We observe  $R(v_2\{4\})$  deviates from unity in the most central isobar collisions, while firm conclusion needs high statistical runs.

In fact,  $ac_2\{3\}$  is largely influenced by individual flow harmonics, while the correspondent normalized asymmetric cumulant  $nac_2\{3\}$  could reduce such flow contributions.  $nac_2\{3\}$  directly reflect the correlation between second and fourth order event-plane  $\langle \cos 4(\Phi_2 - \Phi_4) \rangle$ , after neglecting the correlations between different flow harmonics. In Fig. (3) (a) and (b), we plot the ratios of normalized asymmetric cumulant  $R(nac_2\{3\})$  and  $R(\langle \cos 4(\Phi_2 - \Phi_4) \rangle)$  with  $\Phi_2 = (1/2) \arctan(\text{Im}Q_2/\text{Re}Q_2)$  and  $\Phi_4 = (1/4) \arctan(\text{Im}Q_4/\text{Re}Q_4)$ . We found the event-plane correlations ratio  $R(\langle \cos 4(\Phi_2 - \Phi_4) \rangle)$  also depend on  $\beta_{2,Ru}$  and  $\beta_{3,Zr}$ , which show similar trend as  $R(ac_2\{3\})$  and  $R(v_2\{2\})$  in Fig. 1 and Fig. 2(a). We note that the event plane correlations can also be calculated by [22]

$$c\{2, 2, -4\} \equiv \frac{\langle Q_{2A}^2 Q_{4B}^* \rangle}{\sqrt{\langle Q_{4A} Q_{4B}^* \rangle} \sqrt{\langle Q_{2A}^2 Q_{2B}^* \rangle}} \quad (9)$$

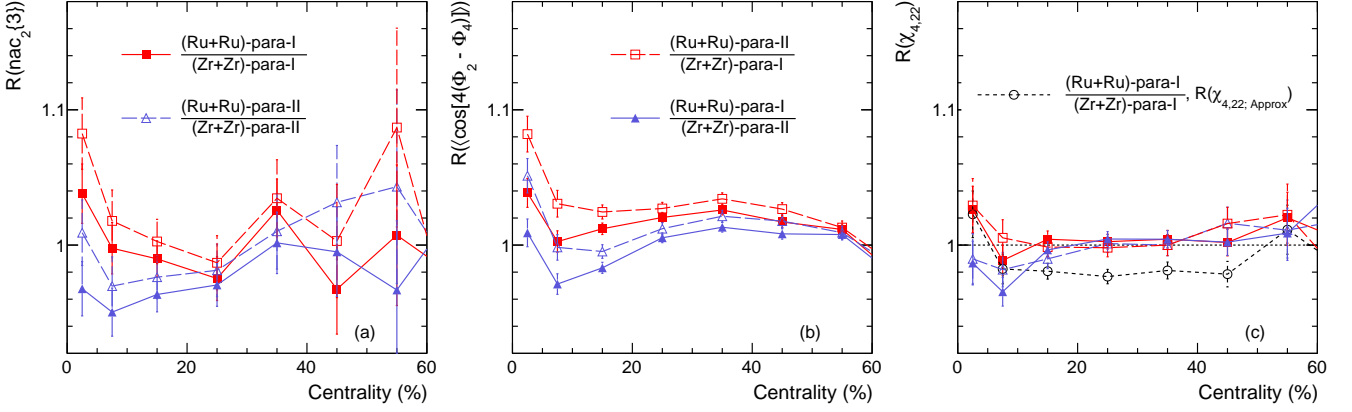


Figure 3: The centrality dependent (a)  $R(\text{nac}_2\{3\})$ , (b)  $R(\langle \cos 4(\Phi_2 - \Phi_4) \rangle)$  and (c)  $R(\chi_{4,22})$  calculated by iEBE-VISHNU model with different sets of nuclear deformations. The approximated  $R(\chi)$  calculated by Eq. (11) is shown as open black circles in (c). The observables are calculated by the standard Q-cumulant method with  $0.2 < p_T < 2$  GeV/c and  $|\eta| < 2$ .

with the two sub-event method, and we have checked that the  $R(c\{2, 2, -4\})$  consist with  $R(\text{nac}_2\{3\})$  and  $R(\langle \cos 4(\Phi_2 - \Phi_4) \rangle)$  within large statistical errors.

It is also interested to study the nonlinear response coefficient  $\chi_{4,22}$  ratios in isobar collisions, which is defined as [24]:

$$\chi_{4,22} \equiv \frac{\text{ac}_2\{3\}}{\langle v_2^4 \rangle} = \text{nac}_2\{3\} \sqrt{\frac{v_4\{2\}^2}{2v_2\{2\}^4 - v_2\{4\}^4}}. \quad (10)$$

The results are shown in Fig. 3(c), which is consist with unity within errors. It indicates that the nonlinear coefficient  $\chi_{4,22}$  is not sensitive to the nuclear deformation, although the top 5% results show some weak sensitivities with large uncertainties. Note that earlier study also found that the nonlinear coefficients are not sensitive to the details of the initial state fluctuations [24].

In the most central collisions, the  $v_2\{4\}$  is significantly smaller than  $v_2\{2\}$ , then  $\chi_{4,22}$  can be approximately expressed as:<sup>1</sup>

$$R(\chi_{4,22;\text{Approx}}) = \frac{\text{ac}_2\{3\}}{v_2\{2\}^4}. \quad (11)$$

Fig. 3(c) also shows  $R(\chi_{4,22;\text{Approx}})$ , calculated with  $\beta_{2,\text{Ru}} = 0.12$  and  $\beta_{3,\text{Zr}} = 0.16$ , with open black circles. We find that this approximation works well for top 10% centrality, but failed at semi-central and peripheral collisions. Such deviation at non-central collisions indicates that fluctuations are essential to understand the flow differences in relativistic isobar collisions.

The similar trends for  $R(\text{ac}_2\{3\})$ ,  $R(\langle \cos 4(\Phi_2 - \Phi_4) \rangle)$ , and  $R(v_2\{2\})$  indicate that both the nuclear deformation and the resulting fluctuations are important to understand the observed flow differences in isobar collisions. In Fig. 4, as a summary, we compare those ratios with two sets of deformations, i.e., (Ru-para-I, Zr-para-I) v.s. (Ru-para-II, Zr-para-II). We find that the  $R(\text{ac}_2\{3\})$ ,  $R(\langle \cos 4(\Phi_2 - \Phi_4) \rangle)$ , and  $R(v_2\{2\})$  show different response to the deformation. We expected that our proposed observables, together with other observables like  $R(v_3)$ , can be

used to constrain the initial deformation and fluctuations for relativistic isobar collisions.

Note that the non-flow contributions have not been fully included in our study, since non-flow contribution from iEBE-VISHNU simulations are mainly from resonance decay. If the non-flow contributions are the same for the two colliding system, the observed differences should be diluted to some extent. We have checked that the  $|\eta| < 2$  used in this study make the  $R(v_2\{2\})$  a little bit larger deviate from unity than the one using a smaller pseudorapidity cut  $|\eta| < 1$ . We also find that the sub-event method (e.g.  $\Delta\eta > 0.4$ ) can also suppress the non-flow effect, which make the  $R(v_2\{2\})$  further deviate from unity. These effects are considerably small on  $R(v_2\{2\})$ , and even not visible on other observables, partly due to large statistical uncertainties. For the three particle cumulant  $\text{ac}_2\{3\}$ , the three sub-event method can largely suppress the non-flow contributions but restricted by statistics. Besides resonance decay, further studies with more non-flow effects included are needed. The dataset collected in the experiment (about 2 billion events for each collision system) [30] is 1.4 times larger than the model study used in this work (about 3million (hydro)  $\times$  50(UrQMD oversamplings) = 150 million events for each collision system), with which observables are expected to be measured more precisely with various non-flow subtraction methods. The comparison between model study and the experiment data can provide more insights on the non-flow contributions.

## 4. Summary

The observed differences between flow harmonics for  ${}^{96}_{44}\text{Ru} + {}^{96}_{44}\text{Ru}$  and  ${}^{96}_{40}\text{Zr} + {}^{96}_{40}\text{Zr}$  collisions at  $\sqrt{s_{\text{NN}}} = 200$  GeV indicates unique opportunities to probe the nuclear structure of the colliding nuclei. In this letter, we proposed that the asymmetric cumulant ratio  $R(\text{ac}_2\{3\})$ , together with the corresponding individual flow harmonic ratios  $R(v_n)$  and event-plane correlation ratio  $R(\text{nac}_2\{3\})$  ( $R(\langle \cos 4(\Phi_2 - \Phi_4) \rangle)$ ), can simultaneously constrain the nuclear deformation and the resulting fluctuations.

<sup>1</sup>We thank G. Giacalone for valuable discussion on this point.

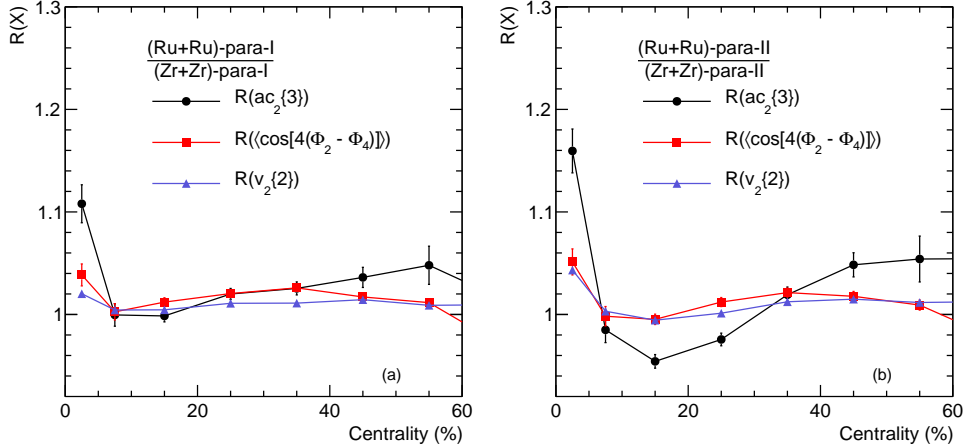


Figure 4: The comparison among  $R(ac_2\{3\})$ ,  $R(\langle \cos[4(\Phi_2 - \Phi_4)] \rangle)$  and  $R(v_2\{2\})$  at relativistic isobar collisions with different set of nuclear deformations: (a) (Ru+Ru)-para-I, (Zr+Zr)-para-I and (b) (Ru+Ru)-para-II, (Zr+Zr)-para-II. The observables are calculated by the standard Q-cumulant method with  $0.2 < p_T < 2$  GeV/c and  $|\eta| < 2$ .

Our iEBE-VISHNU hybrid model simulations indicate that the statistical friendly observable  $R(ac_2\{3\})$  is very sensitive to the quadrupole and octupole deformation of  $\beta_2$  and  $\beta_3$ . To further investigate this sensitivity, we divided the  $ac_2\{3\}$  into three parts, i.e.,  $v_2$  ( $v_2\{2\}$  and  $v_2\{4\}$ ),  $v_4$  ( $v_4\{2\}$ ), and the normalized asymmetric cumulants  $nac_2\{3\}$ , but ignore their correlations and non-flow effect. We found that both the flow harmonics differences and event-plane correlation differences in the isobar collisions depend on  $\beta_{2,Ru}$  and  $\beta_{3,Zr}$ . The event-plane correlation differences on the nuclear structure could be larger than the elliptic flow difference, indicating the importance of initial fluctuations. The  $R(ac_2\{3\}) \approx R(v_2\{2\})^4$  works well in the most central collisions, but show obvious deviation in non-central collisions. We found the nonlinear coefficients extracted from the  $ac_2\{3\}$  are identical in the two systems, indicating the insensitivity to the initial state and the details of nuclear deformation.

## Acknowledgments

We thank G. Giacalone, J. Jia, F. Wang and W. Zhao for useful discussions. We thank Yu Hu for providing the STAR data. This work is supported in part by the National Natural Science Foundation of China (Grant Nos. 12075007, 11905059, 12035006, 12075085), and the Zhejiang Provincial Natural Science Foundation of China (Grant No. LY21A050001).

## References

- [1] J. Adams, et al., Experimental and theoretical challenges in the search for the quark gluon plasma: The STAR Collaboration's critical assessment of the evidence from RHIC collisions, Nucl.Phys. A757 (2005) 102–183. arXiv:nucl-ex/0501009, doi:10.1016/j.nuclphysa.2005.03.085.
- [2] K. Adcox, et al., Formation of dense partonic matter in relativistic nucleus-nucleus collisions at RHIC: Experimental evaluation by the PHENIX collaboration, Nucl.Phys. A757 (2005) 184–283. arXiv:nucl-ex/0410003, doi:10.1016/j.nuclphysa.2005.03.086.
- [3] K. Aamodt, et al., Elliptic flow of charged particles in Pb-Pb collisions at 2.76 TeV, Phys. Rev. Lett. 105 (2010) 252302. arXiv:1011.3914, doi:10.1103/PhysRevLett.105.252302.
- [4] P. Romatschke, U. Romatschke, Viscosity Information from Relativistic Nuclear Collisions: How Perfect is the Fluid Observed at RHIC?, Phys.Rev.Lett. 99 (2007) 172301. arXiv:0706.1522, doi:10.1103/PhysRevLett.99.172301.
- [5] D. A. Teaney, Viscous Hydrodynamics and the Quark Gluon Plasma, 2010, pp. 207–266. arXiv:0905.2433, doi:10.1142/9789814293297\_0004.
- [6] H. Song, S. A. Bass, U. Heinz, T. Hirano, C. Shen, 200 A GeV Au+Au collisions serve a nearly perfect quark-gluon liquid, Phys. Rev. Lett. 106 (2011) 192301, [Erratum: Phys. Rev. Lett.109,139904(2012)]. arXiv:1011.2783, doi:10.1103/PhysRevLett.106.192301, 10.1103/PhysRevLett.109.139904.
- [7] H. Niemi, G. S. Denicol, P. Huovinen, E. Molnar, D. H. Rischke, Influence of the shear viscosity of the quark-gluon plasma on elliptic flow in ultrarelativistic heavy-ion collisions, Phys. Rev. Lett. 106 (2011) 212302. arXiv:1101.2442, doi:10.1103/PhysRevLett.106.212302.
- [8] U. Heinz, R. Snellings, Collective flow and viscosity in relativistic heavy-ion collisions, Ann. Rev. Nucl. Part. Sci. 63 (2013) 123–151. arXiv:1301.2826, doi:10.1146/annurev-nucl-102212-170540.
- [9] H. Song, Y. Zhou, K. Gajdosova, Collective flow and hydrodynamics in large and small systems at the LHC, Nucl. Sci. Tech. 28 (7) (2017) 99. arXiv:1703.00670, doi:10.1007/s41365-017-0245-4.
- [10] M. Gyulassy, I. Vitev, X.-N. Wang, B.-W. Zhang, Jet quenching and radiative energy loss in dense nuclear matter, Hwa. R.C. (ed.) et al., Quark gluon plasma (2003) 123–191 arXiv:nucl-th/0302077.
- [11] P. Kovtun, D. Son, A. Starinets, Viscosity in strongly interacting quantum field theories from black hole physics, Phys.Rev.Lett. 94 (2005) 111601. arXiv:hep-th/0405231, doi:10.1103/PhysRevLett.94.111601.
- [12] B. Schenke, S. Jeon, C. Gale, Elliptic and triangular flow in event-by-event (3+1)D viscous hydrodynamics, Phys. Rev. Lett. 106 (2011) 042301. arXiv:1009.3244, doi:10.1103/PhysRevLett.106.042301.
- [13] H. Song, QGP viscosity at RHIC and the LHC - a 2012 status report, Nucl. Phys. A 904-905 (2013) 114c–121c. arXiv:1210.5778, doi:10.1016/j.nuclphysa.2013.01.052.
- [14] C. Gale, S. Jeon, B. Schenke, P. Tribedy, R. Venugopalan, Event-by-event anisotropic flow in heavy-ion collisions from combined Yang-Mills and viscous fluid dynamics, Phys. Rev. Lett. 110 (1) (2013) 012302. arXiv:1209.6330, doi:10.1103/PhysRevLett.110.012302.
- [15] C. Gale, S. Jeon, B. Schenke, Hydrodynamic Modeling of Heavy-Ion Collisions, Int.J.Mod.Phys. A28 (2013) 1340011. arXiv:1301.5893, doi:10.1142/S0217751X13400113.
- [16] H.-j. Xu, Z. Li, H. Song, High-order flow harmonics of identified hadrons in 2.76A TeV Pb + Pb collisions, Phys. Rev. C93 (6) (2016) 064905. arXiv:1602.02029, doi:10.1103/PhysRevC.93.064905.
- [17] J. E. Bernhard, J. S. Moreland, S. A. Bass, J. Liu, U. Heinz, Applying

- Bayesian parameter estimation to relativistic heavy-ion collisions: simultaneous characterization of the initial state and quark-gluon plasma medium, *Phys. Rev. C* 94 (2) (2016) 024907. [arXiv:1605.03954](#), [doi:10.1103/PhysRevC.94.024907](#).
- [18] S. McDonald, C. Shen, F. Fillion-Gourdeau, S. Jeon, C. Gale, Hydrodynamic predictions for Pb+Pb collisions at 5.02 TeV, *Phys. Rev. C* 95 (6) (2017) 064913. [arXiv:1609.02958](#), [doi:10.1103/PhysRevC.95.064913](#).
- [19] W. Zhao, H.-j. Xu, H. Song, Collective flow in 2.76 A TeV and 5.02 A TeV Pb+Pb collisions, *Eur. Phys. J. C* 77 (9) (2017) 645. [arXiv:1703.10792](#), [doi:10.1140/epjc/s10052-017-5186-x](#).
- [20] A. Bilandzic, R. Snellings, S. Voloshin, Flow analysis with cumulants: Direct calculations, *Phys. Rev. C* 83 (2011) 044913. [arXiv:1010.0233](#), [doi:10.1103/PhysRevC.83.044913](#).
- [21] A. Bilandzic, C. H. Christensen, K. Gulbrandsen, A. Hansen, Y. Zhou, Generic framework for anisotropic flow analyses with multiparticle azimuthal correlations, *Phys. Rev. C* 89 (6) (2014) 064904. [arXiv:1312.3572](#), [doi:10.1103/PhysRevC.89.064904](#).
- [22] R. S. Bhalerao, J.-Y. Ollitrault, S. Pal, Event-plane correlators, *Phys. Rev. C* 88 (2013) 024909. [arXiv:1307.0980](#), [doi:10.1103/PhysRevC.88.024909](#).
- [23] G. Aad, et al., Measurement of long-range pseudorapidity correlations and azimuthal harmonics in  $\sqrt{s_{NN}} = 5.02$  TeV proton-lead collisions with the ATLAS detector, *Phys. Rev. C* 90 (4) (2014) 044906. [arXiv:1409.1792](#), [doi:10.1103/PhysRevC.90.044906](#).
- [24] L. Yan, J.-Y. Ollitrault,  $v_4, v_5, v_6, v_7$ : nonlinear hydrodynamic response versus LHC data, *Phys. Lett. B* 744 (2015) 82–87. [arXiv:1502.02502](#), [doi:10.1016/j.physletb.2015.03.040](#).
- [25] J. Jia, M. Zhou, A. Trzupek, Revealing long-range multiparticle collectivity in small collision systems via subevent cumulants, *Phys. Rev. C* 96 (3) (2017) 034906. [arXiv:1701.03830](#), [doi:10.1103/PhysRevC.96.034906](#).
- [26] X. Zhu, Y. Zhou, H. Xu, H. Song, Correlations of flow harmonics in 2.76A TeV Pb–Pb collisions, *Phys. Rev. C* 95 (4) (2017) 044902. [arXiv:1608.05305](#), [doi:10.1103/PhysRevC.95.044902](#).
- [27] M. Aaboud, et al., Correlated long-range mixed-harmonic fluctuations measured in *pp*, *p*+Pb and low-multiplicity Pb+Pb collisions with the ATLAS detector, *Phys. Lett. B* 789 (2019) 444–471. [arXiv:1807.02012](#), [doi:10.1016/j.physletb.2018.11.065](#).
- [28] C. Zhang, J. Jia, J. Xu, Non-flow effects in three-particle mixed-harmonic azimuthal correlations in small collision systems, *Phys. Lett. B* 792 (2019) 138–141. [arXiv:1812.03536](#), [doi:10.1016/j.physletb.2019.03.035](#).
- [29] M. Li, Y. Zhou, W. Zhao, B. Fu, Y. Mou, H. Song, Investigations on mixed harmonic cumulants in heavy-ion collisions at energies available at the CERN Large Hadron Collider, *Phys. Rev. C* 104 (2) (2021) 024903. [arXiv:2104.10422](#), [doi:10.1103/PhysRevC.104.024903](#).
- [30] M. Abdallah, et al., Search for the chiral magnetic effect with isobar collisions at  $\sqrt{s_{NN}}=200$  GeV by the STAR Collaboration at the BNL Relativistic Heavy Ion Collider, *Phys. Rev. C* 105 (1) (2022) 014901. [arXiv:2109.00131](#), [doi:10.1103/PhysRevC.105.014901](#).
- [31] H.-j. Xu, W. Zhao, H. Li, Y. Zhou, L.-W. Chen, F. Wang, Probing nuclear structure with mean transverse momentum in relativistic isobar collisions [arXiv:2111.14812](#).
- [32] H.-J. Xu, X. Wang, H. Li, J. Zhao, Z.-W. Lin, C. Shen, F. Wang, Importance of isobar density distributions on the chiral magnetic effect search, *Phys. Rev. Lett.* 121 (2) (2018) 022301. [arXiv:1710.03086](#), [doi:10.1103/PhysRevLett.121.022301](#).
- [33] H. Li, H.-j. Xu, J. Zhao, Z.-W. Lin, H. Zhang, X. Wang, C. Shen, F. Wang, Multiphase transport model predictions of isobaric collisions with nuclear structure from density functional theory, *Phys. Rev. C* 98 (5) (2018) 054907. [arXiv:1808.06711](#), [doi:10.1103/PhysRevC.98.054907](#).
- [34] H. Li, H.-j. Xu, Y. Zhou, X. Wang, J. Zhao, L.-W. Chen, F. Wang, Probing the neutron skin with ultrarelativistic isobaric collisions, *Phys. Rev. Lett.* 125 (22) (2020) 222301. [arXiv:1910.06170](#), [doi:10.1103/PhysRevLett.125.222301](#).
- [35] A. Rosenhauer, H. Stocker, J. A. Maruhn, W. Greiner, Influence of shape fluctuations in relativistic heavy ion collisions, *Phys. Rev. C* 34 (1986) 185–190. [doi:10.1103/PhysRevC.34.185](#).
- [36] J. E. Bernhard, J. S. Moreland, S. A. Bass, Bayesian estimation of the specific shear and bulk viscosity of quark–gluon plasma, *Nature Phys.* 15 (11) (2019) 1113–1117. [doi:10.1038/s41567-019-0611-8](#).
- [37] P. Filip, R. Lednicky, H. Masui, N. Xu, Initial eccentricity in deformed Au-197 + Au-197 and U-238 + U-238 collisions at  $s_{NN}=200$  GeV at the BNL Relativistic Heavy Ion Collider, *Phys. Rev. C* 80 (2009) 054903. [doi:10.1103/PhysRevC.80.054903](#).
- [38] G. Giacalone, Observing the deformation of nuclei with relativistic nuclear collisions, *Phys. Rev. Lett.* 124 (20) (2020) 202301. [arXiv:1910.04673](#), [doi:10.1103/PhysRevLett.124.202301](#).
- [39] C. Zhang, J. Jia, Evidence of Quadrupole and Octupole Deformations in Zr96+Zr96 and Ru96+Ru96 Collisions at Ultrarelativistic Energies, *Phys. Rev. Lett.* 128 (2) (2022) 022301. [arXiv:2109.01631](#), [doi:10.1103/PhysRevLett.128.022301](#).
- [40] Q. Y. Shou, Y. G. Ma, P. Sorensen, A. H. Tang, F. Videbæk, H. Wang, Parameterization of Deformed Nuclei for Glauber Modeling in Relativistic Heavy Ion Collisions, *Phys. Lett. B* 749 (2015) 215–220. [arXiv:1409.8375](#), [doi:10.1016/j.physletb.2015.07.078](#).
- [41] H.-j. Xu, H. Li, X. Wang, C. Shen, F. Wang, Determine the neutron skin type by relativistic isobaric collisions, *Phys. Lett. B* 819 (2021) 136453. [arXiv:2103.05595](#), [doi:10.1016/j.physletb.2021.136453](#).
- [42] H.-j. Xu, H. Li, Y. Zhou, X. Wang, J. Zhao, L.-W. Chen, F. Wang, Measuring neutron skin by grazing isobaric collisions, *Phys. Rev. C* 105 (1) (2022) L011901. [arXiv:2105.04052](#), [doi:10.1103/PhysRevC.105.L011901](#).
- [43] J. Jia, Probing triaxial deformation of atomic nuclei in high-energy heavy ion collisions [arXiv:2109.00604](#).
- [44] L.-M. Liu, C.-J. Zhang, J. Zhou, J. Xu, J. Jia, G.-X. Peng, Probing neutron-skin thickness with free spectator neutrons in ultracentral high-energy isobaric collisions [arXiv:2203.09924](#).
- [45] J. S. Moreland, J. E. Bernhard, S. A. Bass, Bayesian calibration of a hybrid nuclear collision model using p-Pb and Pb-Pb data at energies available at the CERN Large Hadron Collider, *Phys. Rev. C* 101 (2) (2020) 024911. [arXiv:1808.02106](#), [doi:10.1103/PhysRevC.101.024911](#).
- [46] C. Shen, Z. Qiu, H. Song, J. Bernhard, S. Bass, U. Heinz, The iEBE-VISHNU code package for relativistic heavy-ion collisions, *Comput. Phys. Commun.* 199 (2016) 61–85. [arXiv:1409.8164](#), [doi:10.1016/j.cpc.2015.08.039](#).
- [47] H. Song, S. A. Bass, U. Heinz, Viscous QCD matter in a hybrid hydrodynamic+Boltzmann approach, *Phys. Rev. C* 83 (2011) 024912. [arXiv:1012.0555](#), [doi:10.1103/PhysRevC.83.024912](#).
- [48] H. Song, U. W. Heinz, Causal viscous hydrodynamics in 2+1 dimensions for relativistic heavy-ion collisions, *Phys. Rev. C* 77 (2008) 064901. [arXiv:0712.3715](#), [doi:10.1103/PhysRevC.77.064901](#).
- [49] H. Song, U. W. Heinz, Suppression of elliptic flow in a minimally viscous quark-gluon plasma, *Phys. Lett. B* 658 (2008) 279–283. [arXiv:0709.0742](#), [doi:10.1016/j.physletb.2007.11.019](#).
- [50] S. A. Bass, et al., Microscopic models for ultrarelativistic heavy ion collisions, *Prog. Part. Nucl. Phys.* 41 (1998) 255–369, [*Prog. Part. Nucl. Phys.* 41, 225 (1998)]. [arXiv:nucl-th/9803035](#), [doi:10.1016/S0146-6410\(98\)00058-1](#).
- [51] M. Bleicher, et al., Relativistic hadron hadron collisions in the ultrarelativistic quantum molecular dynamics model, *J. Phys. G* 25 (1999) 1859–1896. [arXiv:hep-ph/9909407](#), [doi:10.1088/0954-3899/25/9/308](#).
- [52] J. S. Moreland, J. E. Bernhard, S. A. Bass, Alternative ansatz to wounded nucleon and binary collision scaling in high-energy nuclear collisions, *Phys. Rev. C* 92 (1) (2015) 011901. [arXiv:1412.4708](#), [doi:10.1103/PhysRevC.92.011901](#).
- [53] G. Nijs, W. van der Schee, Inferring nuclear structure from heavy isobar collisions using Trajectum [arXiv:2112.13771](#).
- [54] S. Zhao, et al., Extracting the nuclear structure parameters in relativistic isobar collisions.
- [55] J. Wang, et al., Importance of initial fluctuations on anisotropic flow in relativistic isobar collisions.